DOI 10.1007/s10946-024-10221-6
Journal of Russian Laser Research, Volume 45, Number 3, May, 2024

REAL-TIME MONITORING OF LASER-LAYERED PAINT REMOVAL FROM CFRP BASED ON THE SYNERGY OF LASER-INDUCED BREAKDOWN SPECTROSCOPY AND PLS-DA MODELS

Ying Zhao,[1] Xiaoyong Zhuo,[1] Yanqun Tong,[1] Jianyu Huang,[1] Shuai Wang,[1] Wangfan Zhou,[1] Liang Chen,[1] Yu Chen,[1] and Wen Shi[2*]

[1] *Department of Mechanical Engineering*
Jiangsu University
Zhenjiang 212013, China

[2] *College of Electric and Electronic Information Engineering*
Wenzhou University
Wenzhou 325035, China

*Corresponding author e-mail: 953503654@qq.com

Abstract

To achieve precise removal of different coatings from carbon fiber-reinforced polymer (CFRP), we propose real-time monitoring for laser-layered paint removal. Current methods for laser paint removal on CFRP surfaces primarily focus on temperature control to safeguard the CFRP against potential damage, yet encounter challenges in providing real-time monitoring capabilities. In this study, we present laser-induced breakdown spectroscopy (LIBS) combined with partial least-squares discriminant analysis (PLS-DA) models as a promising approach. Initially, in this study, we analyze the elemental composition of carbon fiber substrates, primer, and topcoat to identify key characteristic elements for evaluating the laser-layered paint removal effectiveness. Subsequently, we explore changes in the intensities of characteristic spectral lines associated with the characteristic elements in different layers. Lastly, we develop PLS-DA models to effectively identify and classify the carbon fiber substrates, primer, and topcoat, enabling real-time monitoring of laser-layered paint removal. Based on the measured LIBS characteristic intensities and PLS-DA models, we accurately identified materials using Al I (396.164 nm) and Cr I (428.984 nm), or exclusively Cr I (428.984 nm), with 100% accuracy. The results demonstrate the feasibility of integrating LIBS with PLS-DA for monitoring laser-layered paint removal and show its potential in high-quality surface cleaning and automation.

Keywords: real-time monitoring, laser paint removal, laser-induced breakdown spectroscopy (LIBS), partial least-squares discriminant analysis (PLS-DA), carbon fiber reinforced polymer (CFRP).

1. Introduction

Carbon fiber-reinforced polymer (CFRP) is a novel material extensively employed in aerospace, rail transportation, and military equipment. The surface of CFRP typically features coatings comprising one or more distinct materials [1]. Over time, local damage may occur in CFRP paint layers. For safety

Manuscript submitted by the authors in English on March 15, 2024.

 1071-2836/24/4503-0354©2024 Springer Nature Switzerland AG

reasons, technicians must periodically address the damaged paint layers, restoring the surface with the same material through cleaning and repainting. Laser paint removal, with its advantages of high efficiency, environmental friendliness, safety, and automation, presents a competitive choice for removing damaged paint layers compared to traditional methods [2–4]. Owing to the multiple layers of CFRP coatings and varying degrees of damage during use, fixed-condition laser paint removal may result in substrate damage in some areas and incomplete removal of surface coatings in others [5]. Hence, real-time monitoring of laser-layered paint removal is necessary to ensure the quality and efficiency of the process.

In recent years, laser paint removal has effectively cleared surface paint from Al alloy on aircraft skins [6]. However, research on laser paint removal of CFRP surface paint is rare due to the large anisotropy in thermo-physical properties between its components. Xuan et al. [7] employed an Nd : YAG laser to remove coatings from CFRP laminate and investigated the effects of various parameters on surface temperature, apparent morphology, and mechanical properties. The results demonstrated the feasibility of laser paint stripping technology for CFRP laminate. He et al. [8] developed a numerical model for material removal on a heterogeneous fiber-matrix mesh, simulating the heat transfer process between carbon fiber and resin matrix. Simulation results indicated that, at a matrix temperature of 100° C, the laser ablation depth did not penetrate the full coating thickness. Gu et al. [9] successfully removed multi-layer coatings from the CFRP surface, using a UV picosecond laser, with sample temperature monitored by an infrared thermal imager during the cleaning process. In view of the aforementioned results, the majority of research on laser paint removal of CFRP surface paint centers is based on safeguarding CFRP from potential thermal damage or degradation of mechanical properties through temperature control. Importantly, the practical non-uniformity of the paint layer to be cleaned is a notable factor. Current methods offer fixed parameters but lack real-time monitoring technology for achieving effective cleaning under complex conditions.

Real-time monitoring technology for laser cleaning is primarily categorized into spectral signal detection [10], acoustic signal detection [11], and machine vision detection [12]. Given that acoustic signal detection is significantly influenced by background noise and machine vision detection exhibits suboptimum real-time performance in practical applications, the researchers concentrated on laser-induced breakdown spectroscopy (LIBS) [13]. Sun et al. [14] developed a laser cleaning online monitoring system that integrated LIBS technology to real-time monitoring the quality of laser cleaning. The Pearson coefficient analysis method determined the optimum ablation times for laser cleaning, forming a basis for the automatic optimization control of the process. Li et al. [15] removed the oxide layer from hot-rolled stainless steel, using laser cleaning technology with real-time LIBS monitoring. The results demonstrated that the relative intensity ratio of the Fe I emission line at 520.9 nm and the Cr I emission line at 589.2 nm could serve as a quantitative index for monitoring the cleaning process. Yang et al. [16] employed LIBS technology to monitor laser paint removal for the multi-paint layer on the surface of the aircraft's Aluminum alloy skin. They achieved laser-based layered controlled paint removal by monitoring the characteristic element spectrum and composition change law of the topcoat and primer at the corresponding wavelength position. In summary, while LIBS technology has achieved success in various fields, most studies predominantly integrated LIBS technology with laser cleaning for metal surfaces, with limited research on online monitoring and cleaning of carbon fiber composite materials [17]. Due to the complex composition and varying physical properties of each CFRP coating, further analysis and improvement of real-time monitoring for laser-layered paint removal are necessary to achieve precise removal of different coatings on CFRP.

In this paper, we introduce a real-time monitoring technology for laser-layered paint removal of CFRP

based on LIBS technology and Partial Least Squares Discriminant Analysis (PLS-DA) models. Initially, we identify key characteristic elements for evaluating laser-layered paint removal effectiveness, using a scanning electron microscope (SEM) and X-ray energy dispersive spectrometer (EDS). Subsequently, we measure the spectral line intensities of characteristic elements, using a high-energy nanosecond laser and an echelle spectrograph. To find the correlation between changes in characteristic spectral line intensities and laser paint removal effects, we explored these intensity changes in carbon fiber substrates, primer, and topcoat. Finally, we establish PLS-DA models, using the preprocessed data to demonstrate that the characteristic spectral line intensities can identify and classify the carbon fiber substrates, primer, and topcoat for real-time monitoring of laser-layered paint removal.

2. Experiments and Methods

2.1. Experimental Equipment

In Fig. 1, we illustrate the real-time monitoring technology system for laser-layered paint removal. The system can be divided into three components: the plasma excitation system, inspection system, and control system. The plasma excitation system comprised an Nd : YAG high-energy nanosecond pulsed laser (with a wavelength of 1064 nm, a pulse duration of 12 ns, and a repetition rate of 10 Hz), a focusing lens (with a focal length of 150 mm), and a 3D platform. The detection system included a ME-OPT optical signal collector, a photodiode, a DG645 delay generator (with a delay time of 1 μm), and an echelle spectrograph (Andor Mechelle 5000 with a detection wavelength range of ≈200–875 nm, a resolution of 0.1 nm, and an exposure time of 0.2 s). The control system is a computer equipped with professional software.

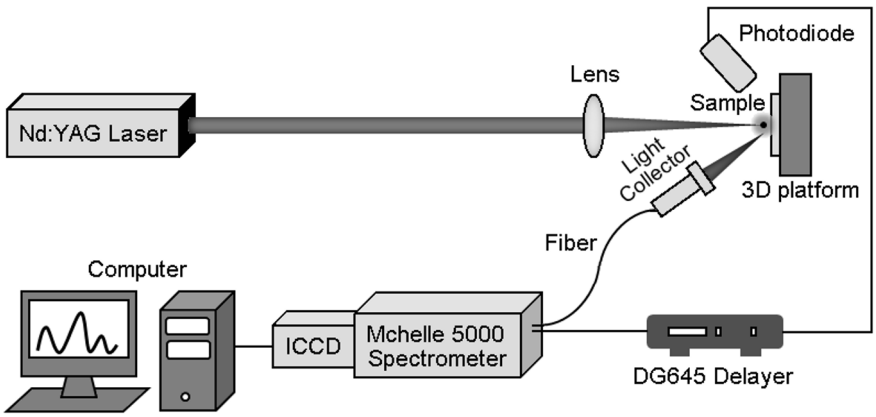

Fig. 1. Laser paint removal online detection system.

During the operation of the real-time monitoring technology for the laser-layered paint removal system, the Nd : YAG laser emitted high-energy pulses interacting with the sample surface through a focusing lens. Then, a bright plasma was induced on the sample surface by the high laser energy density. The plasma light signal was received by a photodiode, triggering a DG645 delay generator to operate an echelle spectrograph. Simultaneously, the plasma optical signal was collected by a ME-OPT optical signal collector and transmitted to an echelle spectrograph via an optical fiber. The echelle spectrograph was utilized to disperse the optical signal. Finally, professional computer software was utilized to display the wavelength and intensity of the plasma spectrum.

2.2. Sample Preparation

The samples utilized in the experiment are carbon fiber-reinforced polymer (CFRP) measuring 40×40 mm. Two paints are adhered to the surface of the CFRP; see Fig. 2. The CFRP substrate, comprised of carbon fiber, features a 20 μm black topcoat composed of polyurethane, and a 50 μm pale yellow primer composed of epoxy resin.

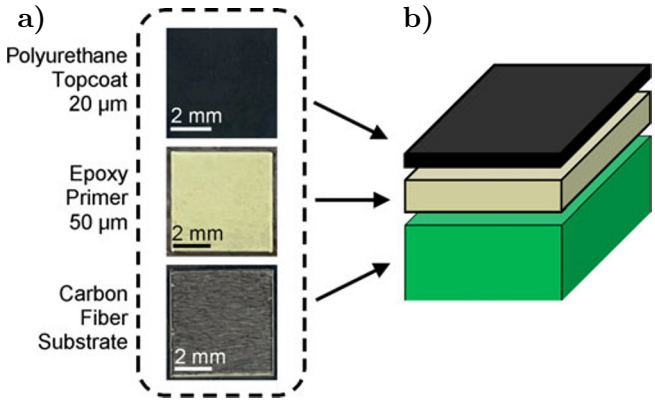

Fig. 2. Carbon fiber reinforced polymer with two layers of paint on the surface; here, the real image of CFRP each layer (a) and sketch map of CFRP (b).

The CFRP surface paints are cleaned by an IPG YLP-HP-100 pulsed fiber laser (with a wavelength of 1064 nm, a maximum output power of 100 W, a pulse duration of 100 ns, a focal spot diameter of 50 μm, and a repetition rate of 80 kHz); see Fig. 3 a. To ensure stable laser operation and optimum beam quality, the laser cleaning system employs a water-cooling method. We observe the surface micromorphology, using a scanning electron microscope (Keyence VK-X260K), and elemental composition analysis is conducted using an X-ray energy dispersive spectrometer (Hitachi S-3400).

We employ univariate analysis to determine the optimum parameters for laser-layered paint removal on CFRP by varying the laser energy density and scanning speed. The analysis indicates that the optimum laser energy density for layered topcoat removal is 15.28 J/cm^2 and, for layered primer removal, it is 34.39 J/cm^2. As shown in Fig. 3 b, the target paint layer can be effectively cleaned without causing damage to the underlying layer. Simultaneously, the optimum scanning speed is 2000 mm/s. Under

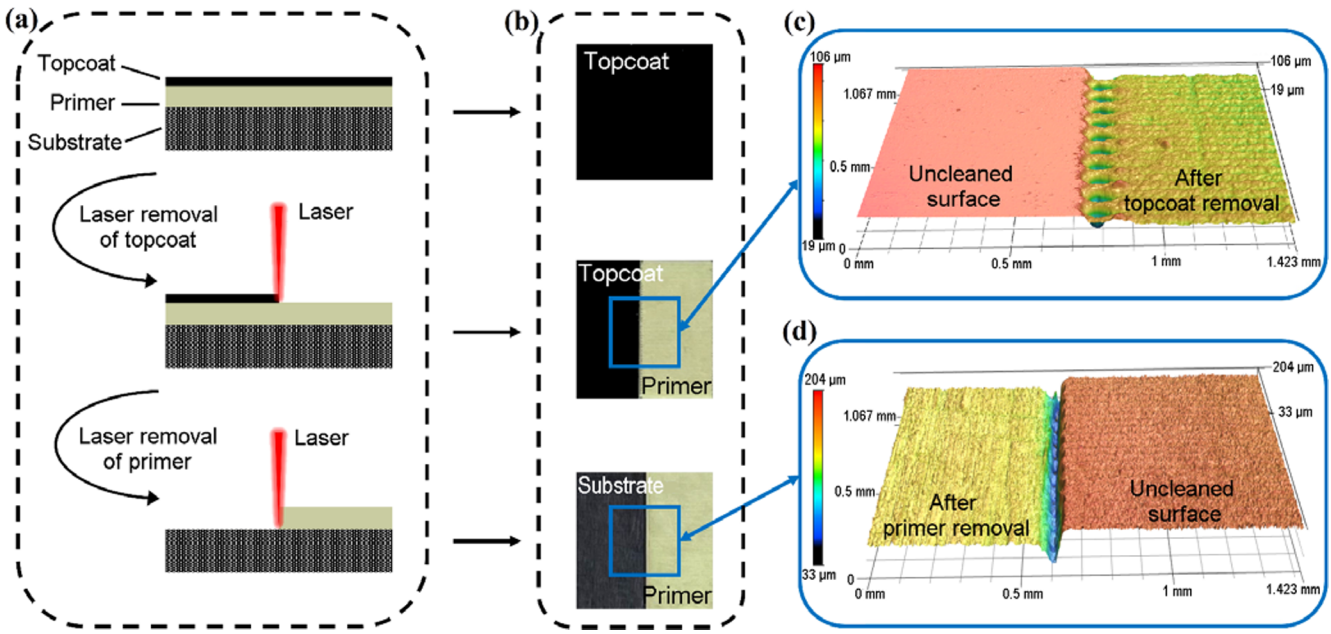

Fig. 3. Three-dimensional topography for laser-layered paint removal of CFRP; here, a sketch map for laser-layered paint removal of CFRP (a), real image of CFRP surface after laser-layered paint removal (b), 3D topography of CFRP after removing topcoat (c), and 3D topography of CFRP after removing primer (d).

these conditions, the topcoat is completely removed with a thickness of 20.56 μm; the primer remains undamaged. At the same scanning speed, the primer is removed without damaging the substrate, with a removed thickness of 50.45 μm. Due to the laser's working mode, the boundary between the laser-affected and non-affected areas is twice scanned by the laser spot, leading to pits with a diameter of ≈50 μm; see Fig. 3 c, d. However, this issue does not impact the online laser paint removal detection system.

2.3. PLS-DA Model

In this study, we employ the partial least squares discriminant analysis (PLS-DA) model, a statistical method primarily for classification and data analysis. PLS-DA improves classification efficiency and accuracy through dimensionality reduction and feature extraction techniques. Accordingly, we maximize the feature differences between categories like carbon fiber substrates, primers, and topcoats, while minimizing the variations within each category. The model aims to efficiently and accurately identify carbon fiber substrates, primers, and topcoats, thereby facilitating real-time monitoring of laser-layered paint removal.

Initially, to normalize the intensity of the characteristic spectral lines, the intensity value at each wavelength is divided by the maximum intensity value in the spectrogram. Subsequently, the spectral line data are transformed into a data set and presented in a matrix format. In this matrix, rows represent elements, and columns represent intensity values corresponding to elements in the spectra. Each row in the matrix represents an independent sample for the statistical analysis of the model. Finally, the samples are divided into calibration and validation sets, with the latter used to assess the predictive performance of the PLS-DA model and to establish evaluation criteria.

The accuracy of the validation set serves as an indicator of the model's sensitivity. A high correct recognition rate corresponds to a low error rate and non-recognition rate, reflecting a heightened sensitivity of the model.

3. Results and Discussion

3.1. CFRP Layered Elemental Composition Analysis

Scanning electron microscope (SEM) images of the carbon fiber reinforced polymer (CFRP) topcoat, primer, and carbon fiber substrate are presented in Fig. 4, a–c. The images distinctly show the morphological differences between the carbon fiber substrate and the two paint layers – the carbon fiber substrate exhibits fine, evenly spaced stripes, whereas the paint layers appear relatively smooth.

We analyze the elemental composition of the CFRP paints and substrate, using an X-ray energy dispersive spectrometer (EDS). Elemental identification and quantification in EDS are achieved by matching the positions of peaks in the spectrum to specific elements, with the intensity of each peak indicating the concentration of the corresponding element. In the analysis of Fig. 4 b, the CFRP topcoat primarily consists of elements, such as C, O, Si, Ba, and S, among others, with the highest intensity for C, followed by Ba, O, Si, Au, and S. Similarly, in Fig. 4 d, we show that the CFRP primer is predominantly composed of C, O, Si, Cr, and Al, among other elements, with C again having the highest intensity, followed by Si, O, Cr, Au, and Al. In Fig. 4 f, C is observed to have the highest abundance, followed by O.

Based on the analysis above, it is evident that both the topcoat and primer, as well as the substrate, contain C and O elements, while the primer uniquely includes elements, such as Cr, Al, Ti, and Sr, with

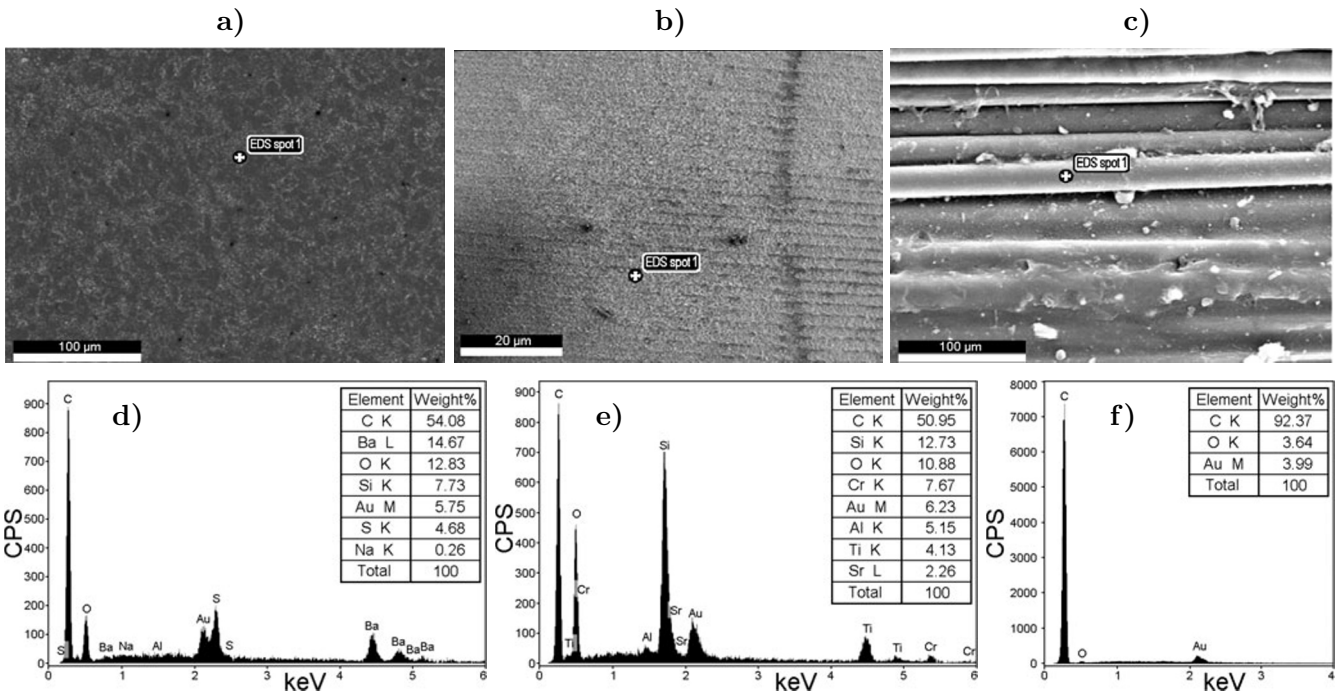

Fig. 4. The diagram of SEM and point energy spectrum analysis. Here, SEM of topcoat (a), energy spectrum analysis of topcoat (b), SEM of primer (c), energy spectrum analysis of primer (d), SEM of substrate (e), and energy spectrum analysis of substrate (f).

the intensities of Cr and Al being higher than those of Ti and Sr. Hence, Cr and Al are identified as key characteristic elements for assessing the effectiveness of laser-layered paint removal.

3.2. Laser-Induced Breakdown Spectrum Analysis

To find the correlation between changes in characteristic spectral line intensities and laser paint removal effects, LIBS spectral data are acquired for the CFRP topcoat, primer, and substrate, using a single-pulse energy of 100 mJ. A high-energy pulsed laser beam is directed at the sample surface, inducing plasma generation as the power density surpassed the ablation threshold. The required characteristic spectral lines of elements are produced during plasma cooling.

The experiment takes place in an ambient air environment, and the surface of the CFRP is not flat. An air breakdown occurs when the high-energy pulse laser interacts with the material. Consequently, the collected laser-induced plasma spectra include characteristic spectral lines of air. The air plasma spectrum predominantly features elemental spectral lines of O and N, concentrated primarily between 700 and 850 nm [18]. The air breakdown has no impact on collecting elemental spectral lines with wavelengths between 350 and 700 nm. To enhance the reliability of experimental conclusions, we exclusively analyze spectral lines with wavelengths from 350 to 440 nm.

After removing the interference of environmental air factors, the LIBS spectra of CFRP are collected; see Fig. 5. The characteristic peak intensity at 396.164 nm for Al and 428.984 nm for Cr is extracted. In Fig. 5 b, the intensity of the characteristic spectral line for Al I (396.164 nm) in the CFRP topcoat is approximately 14.1749 counts, while the intensity of the characteristic spectral line for Cr I (428.984 nm) in the CFRP topcoat is around 13.7664 counts. In Fig. 5 c, the intensity of the characteristic spectral

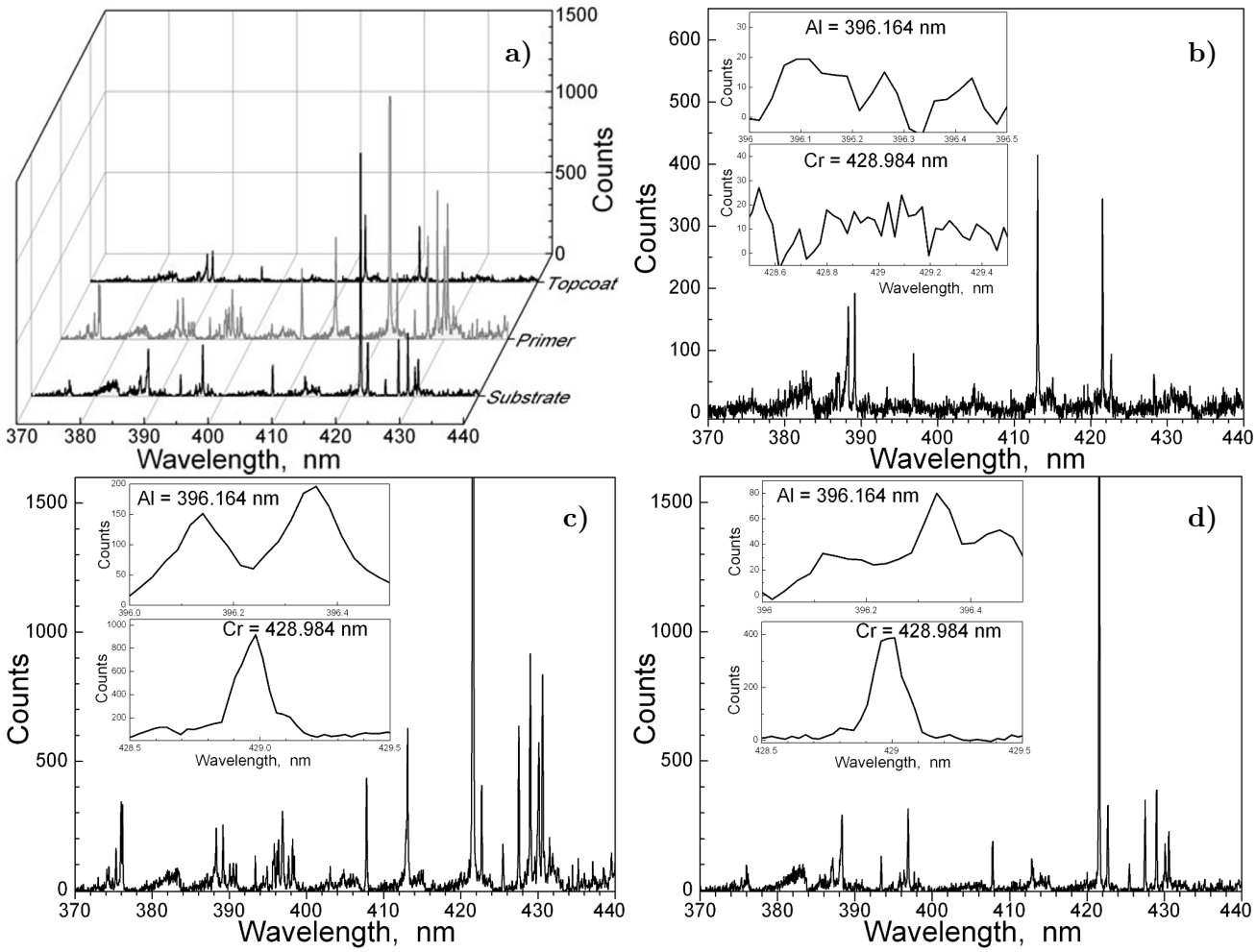

Fig. 5. The LIBS spectra of the CFRP topcoat, primer, and substrate. Here, comparison chart of topcoat, primer, and substrate (a), spectra of topcoat (b), spectra of primer (c), and spectra of substrate (d).

line for Al I (396.164 nm) in the CFRP primer is 122.402 counts and, for Cr I (428.984 nm), it is 917.114 counts. In Fig. 5 d, the intensity of the characteristic spectral line for Al I (396.164 nm) is 28.5724 counts and, for Cr I (428.984 nm), it is approximately 385.677 counts in the CFRP topcoat. The CFRP substrate similarly lacks Al and Cr elements, yet the intensity of the characteristic spectral line in the CFRP substrate is marginally higher than that in the CFRP topcoat. This discrepancy may be attributed to laser action during the laser removal of primer paint, resulting in the partial remelting and adhesion of primer to the carbon fiber substrate. Then, the LIBS laser penetrates the carbon fiber substrate, producing a minimum amount of characteristic spectral line signals for Al and Cr. Nevertheless, this potential error does not compromise real-time monitoring for laser-layered paint removal.

In order to minimize the accidental error in a single experiment, we gather 35 sets of LIBS spectral data for the CFRP topcoat, primer, and carbon fiber substrate; see Fig. 6. The intensities of elemental spectral lines for each CFRP layer are generally aligned on the same horizontal line, confirming the insignificance of data errors. The intensity of the characteristic spectral line in the primer is distinctly different from that in the other two layers; see Fig. 6 a, c. In Fig. 6 b, d, the average spectral line intensity

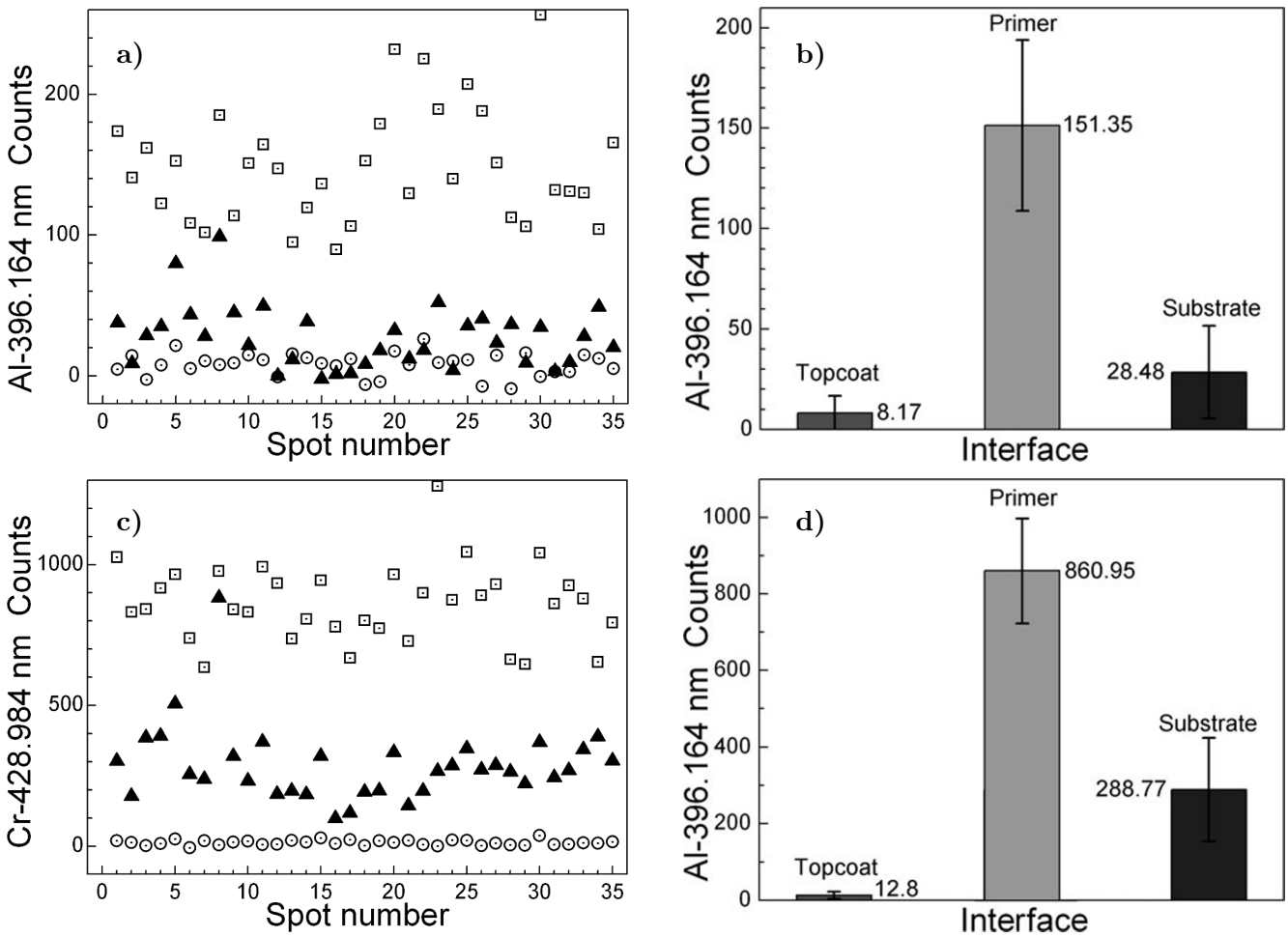

Fig. 6. Statistics of element spectral line intensities: spectral line intensity distributions of topcoat (⊙), primer (□), and substrate (▲) (a, c) and average value of element spectral line intensity of topcoat, primer, and substrate (b, d) for 369.164 nm Al (a, b) and 428.984 nm Cr (c, d).

for Al I (396.164 nm) is approximately 151 counts, and for Cr I (428.984 nm), it is around 860 counts. The average spectral line intensity of Al I (396.164 nm) and Cr I (428.984 nm) in the primer significantly exceeds that in the topcoat and substrate.

Consequently, the changes in spectral line intensities of Al I (396.164 nm) and Cr I (428.984 nm) accurately reflect the effectiveness of laser-layered paint removal. During topcoat removal, the intensities of Al I (396.164 nm) and Cr I (428.984 nm) are relatively low. When the topcoat is completely removed, exposing the primer, the intensities of these lines increase. Further primer removal, exposing the carbon fiber substrate, leads to a decrease of the intensities of Al I (396.164 nm) and Cr I (428.984 nm) once again.

3.3. PLS-DA Model Analysis

To identify and classify carbon fiber substrates, primer, and topcoat based on the intensities of Al I (396.164 nm) and Cr I (428.984 nm), and to realize real-time monitoring of laser-layered paint removal

from CFRP, we develop PLS-DA models, using the acquired spectral data. A total of 105 LIBS spectral data sets are examined, with 80 assigned to Calibration Sets and the remaining 25, to Validation Sets.

We develop three PLS-DA models, using spectral data. The model cross-validation error and validation model PLS-DA load plot are shown in Fig. 7. In the type 1 modeling, Al I (396.164 nm) and Cr I (428.984 nm) are utilized as characteristic spectral lines for analysis. According to Fig. 7 a, b, the number of potential variables selected is 3, enabling complete differentiation of the primer from the topcoat and substrate, as confirmed by verifying the model load figure. The classification results are excellent, with a 100% accuracy rate in the validation set for all cases. The type 2 modeling employs only Cr I (428.984 nm) as the characteristic spectral line for analysis. The number of potential variables selected is equal to 3, yielding the same effectiveness as the type 1 modeling, with a 100% accuracy rate in the validation set. In the type 3 modeling, Al I (396.164 nm) is used as the characteristic spectral line. The number of potential variables selected is 2, leading to only partial distinction among primer, topcoat, and substrate. The classification results are moderate, with validation set accuracies of 85.4%, 100%, and 55.6%. The subpar classification effect when using Al I (396.164 nm) as the analyzed spectral line is attributed to the low Al content in the primer, leading to reduced intensity of Al spectral lines and affecting the model's classification accuracy.

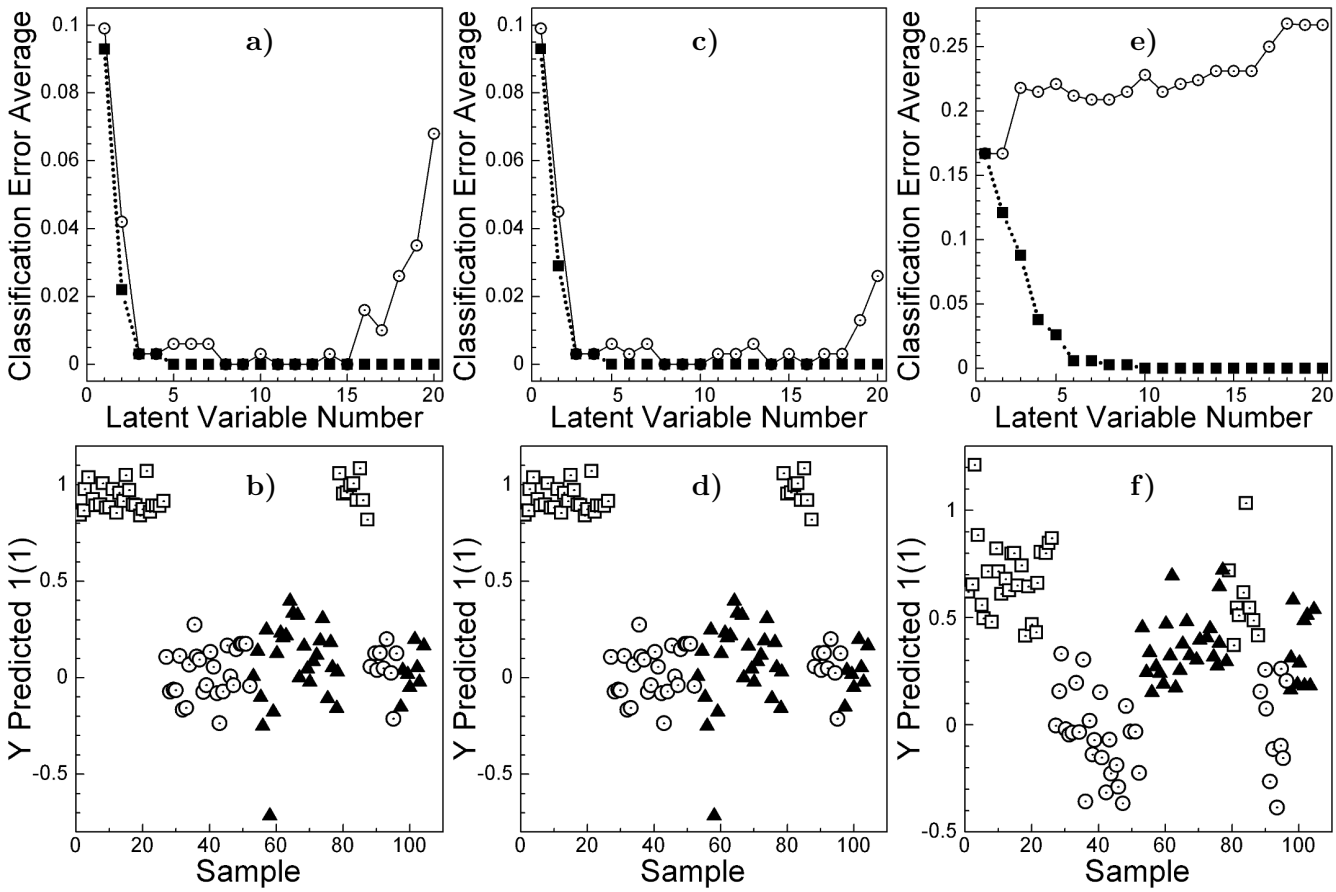

Fig. 7. Model cross-validation (⊙) and calculated (■) errors (a, c, e) and validation model PLS-DA load plots (b, d, f) (topcoat ⊙, primer □, and substrate ▲) for type 1 modeling (a, b), for type 2 modeling (c, d), and for type 3 modeling (e, f).

The three modeling results lead to the conclusion that employing Al I (396.164 nm) with Cr I (428.984 nm) analytical line spectra, as well as using only Cr I (428.984 nm) analytical line spectra, effectively discriminates the analysis of topcoat, primer, and substrate. These two methods of analysis accurately assess the impact of laser-layered paint removal, whereas utilizing only Al I (396.164 nm) analytical line spectra lacks sufficient accuracy for precise predictions.

4. Summary

In this paper, we presented a real-time monitoring technology for laser-layered paint removal from CFRP, employing laser-induced breakdown spectroscopy (LIBS) and partial least squares discriminant analysis (PLS-DA). Initially, we utilized a scanning electron microscope (SEM) and an X-ray energy dispersive spectrometer (EDS) to identify key characteristic elements, Al and Cr, in CFRP. Subsequently, we focused a high-energy pulsed laser beam on the sample surface to generate the required characteristic spectral lines of the elements. The changes in spectral line intensities of Al I (396.164 nm) and Cr I (428.984 nm) accurately reflected the effectiveness of laser-layered paint removal. Lastly, the characteristic spectral line data were preprocessed through normalization, followed by the development of PLS-DA models, using this data. We analyzed three different modeling results. The type 1 modeling utilized both Al I (396.164 nm) and Cr I (428.984 nm) spectral lines, the type 2 modeling employed only Cr I (428.984 nm), and the type 3 modeling used only Al I (396.164 nm). The validation sets for both type 1 and type 2 modeling achieved 100% accuracy.

In summary, the effectiveness of laser-layered paint removal for CFRP can be accurately assessed using Al I (396.164 nm) and Cr I (428.984 nm), or a single Cr I (428.984 nm), with 100% accuracy. In this study, we proposed a technical method for real-time monitoring of laser-layered paint removal from CFRP, providing significant insights for integrated and intelligent modern laser paint removal applications.

Acknowledgments

The authors acknowledge the financial support provided within the National Natural Science Foundation of China under Grant No. 51975261, and the Natural Science Foundation of Jiangsu Province under Grant No. BK20200912.

References

1. I. Ligabo, R. Siqueira, C. Ferreira, et al., *Opt. Laser Technol.*, **143**, 107304 (2021).
2. W. F. Yang, Z. R. Qian, Y. Cao, et al., *Spectrosc. Spectr. Anal.*, **41**, 3233 (2021).
3. M. Q. Zhang, H. X. Dai, Y. H. Zheng, et al., *Appl. Laser*, **40**, 644 (2020).
4. J. J. Xu, M. Jiang, Y. X. Ren, et al., *Opt. Technol.*, **49**, 34 (2023).
5. J. Lee and K. Watkins, *Opt. Lasers Eng.*, **34**, 429 (2000).
6. S. L. Li, S. H. Gao, Z. Qian, et al., *Laser Phys.*, **33**, 105701 (2023).
7. S. Y. Xuan, *New Chem. Mater.*, **48**, 124 (2020).
8. H. Yang, H. Liu, R. Gao, et al., *Opt. Laser Technol.*, **145**, 107450 (2022).
9. J. Gu, X. Su, Y. Jin, et al., *J. Manuf. Process.*, **85**, 272 (2023).
10. L. Chen, G. L. Deng, G. Y. Feng, et al., *Spectrosc. Spectr. Anal.*, **38**, 367 (2018).
11. W. F. Zou and J. Xiong, *J. Gannan Norm. Coll.*, **31**, 43 (2010).
12. T. Y. Shi, L. Z. Zhou, C. M. Wang, et al., *Chin. J. Lasers*, **46**, 83 (2019).

13. Y. Li, Z. Y. Wu, D. P. Chu, et al., *Infrared Laser Eng.*, **52**, 50 (2023).
14. L. X. Sun, W. J. Wang, L. F. Qi, et al., *Chin. J. Lasers*, **47**, 299 (2020).
15. X. Li and C. Guan, *Metals*, **11**, 790 (2021).
16. Y. Q. Tong, Q. H. Lu, J. Z. Zhou, et al., *Spectrosc. Spectr. Anal.*, **40**, 255 (2020).
17. W. J. Wang, L. X. Sun, Y. Lu, et al., *Opt. Laser Technol.*, **145**, 107481 (2022).
18. Y. Q. Tong, A. Zhang, Y. H. Fu, et al., *Spectrosc. Spectr. Anal.*, **39**, 2388 (2019).